Journal of Materials Chemistry A

Accepted Manuscript

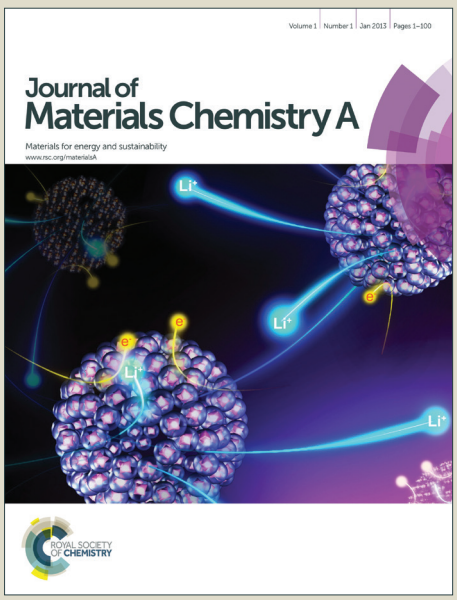

ROYAL SOCIETY OF CHEMISTRY

www.rsc.org/materialsA

Formation of copper vanadate nanobelts and the electrochemical behaviors for the determination of ascorbic acid

Lizhai Pei*, Nan Lin, Tian Wei, Handing Liu and Haiyun Yu

Copper vanadate nanobelts have been successfully synthesized by a facile hydrothermal process using sodium vanadate and copper acetate as the raw materials, polymer polyvinyl pyrrolidone (PVP) as the surfactant by adjusting pH value. The nanobelts are characterized by X-ray diffraction (XRD), scanning electron microscopy (SEM), transmission electron microscopy (TEM) and high-resolution TEM (HRTEM). XRD and HRTEM show that the copper vanadate nanobelts are composed of single crystalline monoclinic $Cu_{2.33}V_4O_{11}$ phase. SEM observation shows that the copper vanadate nanobelts have the thickness, width and length of about 50 nm, 300 nm-1 μm and several tens of micrometers, respectively. pH value plays a key role in the formation of the copper vanadate nanobelts. The growth process of the copper vanadate nanobelts has been proposed as the nucleation and PVP adsorption growth mechanism under acidic and alkaline conditions. The copper vanadate nanobelts have been used as glassy carbon electrode (GCE) modified materials for the determination of ascorbic acid showing good electrochemical detection performance. The linear range is 0.001-2 mM and detection limit is 0.14 μM and 0.38 μM for cvp1 and cvp2, respectively. The copper vanadate nanobelts modified GCE exhibits good stability and reproducibility.

* *Key Lab of Materials Science and Processing of Anhui Province, School of Materials Science and Engineering, Anhui University of Technology, Ma'anshan, Anhui 243002, P. R. China. E-mail: lzpei@ahut.edu.cn, lzpei1977@163.com; Fax: +86-555-2311570; Tel: +86-555-2311570*

A Introduction

Ternary one-dimensional (1D) metal vanadate nanomaterials exhibit good physical and chemical properties with promising application potential in the fields of electrochemical sensors, phocatalysis, high energy lithium batteries and magnetic devices.[1] Indium vanadate nanotube arrays,[2] silver vanadate nanowires[3] and bismuth vanadate nanowires[4] have been synthesized by a simple hydrothermal process using different vanadate and metal salts as the raw materials. In our previous research, single crystalline calcium vanadate nanorods with sheaf-shaped structure were synthesized via the facile hydrothermal route using calcium acetate and sodium vanadate as the raw materials without any surfactants.[5] Manganaese vanadate nanosheets were also synthesized by us by the hydrothermal process exhibiting good visible light photocatalytic properties for the degradation of methyl blue.[6] Manganese vanadate nanobelts with MnV_2O_6 phase have been synthesized using manganase chloride and vanadium oxide as the raw materials at 180℃ for 192 h via the hydrothermal route.[7] Singh *et al.*[8] reported the formation of the silver vanadate nanorods via room temperature wet chemical process without any templates or surfactants using silver nitrate and ammonium vanadate as the raw materials.

Among ternary metal vanadates, copper vanadate shows great application potential in the fields of high energy lithium batteries and electrochemical sensors owing to good electrochemical properties, high discharge capacity and energy density.[9] Generally, bulk copper vanadate with CuV_2O_6 phase can be prepared by high temperature solid phase reaction of V_2O_5 and $Cu(NO_3)_2$,[10] soft chemistry method using V_2O_5 hydrogel and Cu_2O powder.[11] However, to date, ternary 1D copper vanadate nanomaterials are few reported. Recently, Wu *et al.*[12] reported that ε-$Cu_{0.95}V_2O_5$ hollow microspheres and α-CuV_2O_6 nanograins were synthesized via a facile soft chemical method between $V(IV)O(acac)_2$ and copper nitrate in the solution containing polymer polyvinyl pyrrolidone (PVP). Copper vanadate nanobelts with CuV_2O_6 phase

were prepared via a homogeneous reaction between peroxovanadic acid and copper acetate. The peroxovanadic acid was produced from V_2O_5 and H_2O_2.[13] Copper vanadate nanowires with α-CuV_2O_6 phase were synthesized by the hydrothermal reaction of $CuCl_2$ and NH_4VO_3.[14] The copper vanadate nanomaterials are promising cathode candidates for primary lithium batteries used in long-term implantable cardioverter defibrillators (ICD). Besides cathode candidates for primary lithium batteries, metal vanadates have also shown great application potential in electrochemical sensors owing to good electrochemical properties which may be attributed to high-specific capacity and special crystal structure. In particular, 1D vanadate nanomaterials attract special interest because 1D vanadate nanomaterials on glassy carbon electrode (GCE) surface may mediate the heterogeneous oxidation or reduction reaction of biological molecules. In our previous research, manganese vanadate nanorods were used as the GCE modified materials for the electrochemical analysis of L-cysteine.[15] The manganese vanadate nanorods modified GCE showed lower detection limit and wider linear range. The calcium vanadate nanorods modified GCE was used for the electrochemical determination of tartaric acid.[16] The detection limit was 2.4 μM and linear range was 0.005-2 mM.

Ascorbic acid is water soluble and used to prevent or treat some disease. It is also necessary to human metabolism processes, such as inducing differentiation of cells, involving in immune cell functions and immune responses and enhancing iron uptake in human intestinal cells.[17,18] Therefore, it is essential to develop novel GCE modified materials for the electrochemical detemination of ascorbic acid under complex conditions. The copper vanadate nanostructures further enlarge the specific surface area and quantity of active sites to obtain impressive sensitivity. In the paper, copper vanadate nanobelts have been synthesized via a hydrothermal process using sodium vanadate and copper acetate as the raw materials, PVP as the surfactant by adjusting the pH value. The formation process of the copper vanadate nanobelts

has been analyzed based on the morphology of the products obtained from different hydrothermal conditions. The copper vanadate nanobelts have been used as the GCE modified materials to analyze the electrochemical responses of ascorbic acid. The copper vanadate nanobelts modified GCE exhibits low detection limit and wide linear range. The good analytical performance makes the copper vanadate nanobelts promising materials for the electrochemical sensors to detect ascorbic acid.

B Experimental

Na_3VO_4 (AR grade) and $Cu(CH_3COO)_2{\cdot}H_2O$ (AR grade) were purchased from Aladdin Reagent Co., Ltd. of P. R. China and Sinopharm Chemical Reagent Co., Ltd. of P. R. China, respectively. All raw materials were used without further purification. In a typical process, 0.108 g $Cu(CH_3COO)_2{\cdot}H_2O$, 0.2 g Na_3VO_4 and PVP with definite concentrations were dissolved into 60 mL distilled water. Hydrochloric acid was used to adjust the pH value from 2 to 12. Then the mixture was placed into an autoclave with the volume of 100 mL. The autoclave was maintained at 80 to 180 ℃ for 0.5 to 24 h. The experimental parameters are listed in Table 1. Subsequently the autoclave was cooled naturally in air. The dark green precipitates were filtered, washed with distilled water and alcohol for several times and dried at 60 ℃ in air. Finally, the dark green copper vanadate nanobelts powders were obtained.

X-ray diffraction (XRD) patterns of the samples were performed on a Bruker AXS D8 X-ray diffractometer equipped with a graphite monochromatized Cu-Kα radiation (λ=1.5406 Å). The samples were scanned at a scan rate of 0.05 $°s^{-1}$ in the 2θ range of 20-80°. Scanning electron microscopy (SEM) observation was carried out using nova nanoSEM FEI 430 SEM equiped with an energy dispersive spectrometer (EDS). Transmission electron microscopy (TEM) and high-resolution TEM (HRTEM) samples were prepared by putting several drops of solution with copper vanadate nanobelts onto a standard copper grid with a porous carbon film after the samples were dispersed into distilled water and treated for

about 10 min using supersonic wave apparatus. TEM and HRTEM observations were performed using JEOL JEM-2100 TEM operating with 1.9Å point-to-point resolution and a 200-kV accelerating voltage with a GATAN digital photography system.

The copper vanadate nanobelts suspension was prepared by dispersing 10 mg copper vanadate nanobelts in 10 mL dimethylformamide (DMF) solvent with sufficient ultrasonication for about 1 h until a uniform nanobelts suspension was obtained. Prior to the modification, a GCE with the diameter of 3 mm was polished to a mirror using polish paper and alumina pastes of 0.5 μm, and cleaned in an ultrasonic cleaner with alcohol and water sequentially. A copper vanadate nanobelt modified GCE was prepared by coating 10 μL nanobelts suspension on the surface of the bare electrode and allowed to evaporate liquid at room temperature. Ascorbic acid was purchased from Sinopharm Chemical Reagent Co., Ltd. of P. R. China which was analytical grade. Electrochemical (EC) measurement was performed in a model CHI604D electrochemical working station. The copper vanadate nanobelts modified GCE served as the working electrode, a platinum plate and saturated calomel electrode (SCE) served as the counter electrode and reference electrode, respectively. All potentials were with respect to SCE. Cyclic voltammograms (CVs) were recorded in the potential range from -1.0 V to +1.0 V at a potential scan rate of 50 mVs^{-1} in the mixed solution of 0.1 M KCl and ascorbic acid with different concentrations. Electrochemical impedance spectroscopy (EIS) was performed at an amplitude of 10 mV in the frequency range from 4 kHz to 200 Hz with $Fe(CN)_6^{3-}$ as a probe. All measurements were carried out at room temperature.

C Results and discussion

Fig. 1 shows the XRD pattern of the copper vanadate products obtained from 180℃ for 24 h using sodium vanadate and copper acetate as the raw materials with 3wt.% PVP and pH value of 2. All diffraction peaks can be indexed to the monoclinic $Cu_{2.33}V_4O_{11}$ phase (JCPDS card, PDF No. 54-1241). The absence of the

peaks from other phases shows high purity of the copper vanadate products.

The morphology, size and structure of the copper vanadate nanobelts are further illustrated by SEM, TEM and HRTEM. Fig. 2 shows the SEM images of the copper vanadate nanobelts obtained from 180℃ for 24 h using 3wt.% PVP and pH=2. Low-magnification SEM image (Fig. 2(a)) reveals that the products consist entirely of a large amount of free-standing belt-shaped morphology with the length of several tens of micrometers. No other nanostructures are observed from the SEM image. Higher magnification SEM image (Fig. 2(b)) shows that the typical thickness and width of the copper vanadate nanobelts are about 50 nm and 300 nm-1 μm, respectively. The facets of the copper vanadate nanobelts are apparently distinguishable. Each copper vanadate nanobelt has uniform width and smooth surface. EDS spectrum was used to analyze the composition of the copper vanadate nanobelts (Fig. S1 in *Electronic Supplementary Information*). From Fig. S1, it is shown that the nanobelts are composed of Cu, V and O. The atomic ratio of Cu, V and O is about 2.3: 4: 11 which is close to the composition ratio of the $Cu_{2.33}V_4O_{11}$ phase. The result further shows that the copper vanadate nanobelts are composed of $Cu_{2.33}V_4O_{11}$ phase.

The copper vanadate nanobelts can be further confirmed by TEM observation (Fig. 3(a)). A typical facet of single copper vanadate nanobelt is obviously observed which is totally same to that observed by SEM. The typical thickness and width of the copper vanadate nanobelts are about 50 nm and 1 μm, respectively. The nanobelts have smooth surface, uniform width and thickness. The HRTEM image (Fig. 3(b)) shows that the nanobelts have clear parallel fringe indicating good single crystalline nature. The fringe spacing is determined to be 0.75 nm which is same to the lattice spacing of {200} plane of $Cu_{2.33}V_4O_{11}$. The clear and regular lattice fringes show that the copper vanadate nanobelts consist of good single crystalline $Cu_{2.33}V_4O_{11}$ phase.

Similar to the nanobelts with different compositions,[19-21] special growth conditions are required to

synthesize regular copper vanadate nanobelts. In order to analyze the role of pH value on the morphology and structure of the copper vanadate products, the experiments with the pH value of 5, 7, 9 and 12 were carried out. The hydrothermal temperature and duration time were 180℃ and 24 h, respectively. Sodium vanadate, copper acetate and 3wt.% PVP were used as the raw materials. Fig. S2 (*Electronic Supplementary Information*) shows the SEM images of the products obtained from the pH value of 7. Different from the copper vanadate nanobelts, the products are totally composed of rod-shaped morphology with sub-microscale size (Fig. S2(a)). The length and diameter of the copper vanadate microrods are 2-6 μm and 100-300 nm, respectively (Fig. S2(b)). The results show that pH value plays a key role in the formation of the copper vanadate nanobelts. Fig. 4 indicates the SEM images of the copper vanadate nanobelts obtained from 180℃ for 24 h with the pH value of 5, 9 and 12, respectively. It is observed that the products are still composed of copper vanadate nanobelts with the pH value increasing from 5 to 12. The thickness and length of the nanobelts are about 50 nm and several tens of micrometers, respectively. The width of the nanobelts is 250-600 nm, 250-500 nm and 200 nm-1 μm when the pH value is 5, 9 and 12, respectively.

pH value of the hydrothermal solution plays an important effect in the structure of the nanobelts with different compositions.[22] The XRD patterns of the copper vanadate products obtained from different pH values are analyzed so as to research the role of the pH value on the phase of the copper vanadate products. The XRD patterns are shown in Fig. 5. It is observed that the copper vanadate nanobelts obtained from different pH values have same monoclinic $Cu_{2.33}V_4O_{11}$ phase (Figs. 5(a), 5(b), 5(d) and 5(f)). The phase of the copper vanadate microrods obtained from netural hydrothermal solution is very different from that of the nanobelts obtained from acidic or alkaline soultion. The diffraction peaks are assinged to be monoclinic $Cu_5V_2O_{10}$ phase (JCPDS card, PDF No. 33-0504) (Fig. 5(c)). Close observation of the XRD pattern of the

copper vanadate nanobelts prepared at pH=2 reveals the possible coexistent of the peaks of monoclinic $Cu_5V_2O_{10}$ and monoclinic $Cu_{2.33}V_4O_{11}$. However, the diffraction peaks at around 2θ=24.3°, 25.5° and 46.6° are due to the $(\bar{4}01)$, (110) and $(\bar{6}03)$ planes of the monoclinic $Cu_{2.33}V_4O_{11}$ phase (JCPDS card, PDF No. 54-1241). Therefore, it is considered that the morphology of the copper vanadate is closely relative to the structure of the copper vanadate. The morphology difference of the copper vanadate may originate from the difference of the copper vanadate phase. Hydrogen ions or hydroxyl ions may promote the phase change of the products from monoclinic $Cu_5V_2O_{10}$ (microrods) to monoclinic $Cu_{2.33}V_4O_{11}$ phase (nanobelts).

The copper vanadate nanobelts have been synthesized easily via the facile hydrothermal process by adjusting the pH value of the hydrothermal solution. Hydrothermal conditions, such as PVP concentration, hydrothermal temperature and duration time have important effects in the formation and growth of the nanobelts which has been confirmed by other literatures.[23,24] To investigate the formation mechanism of the copper vanadate nanobelts, comparative experiments using different hydrothermal conditions were carried out. pH value is determined to be 2. Fig. S3 (*Electronic Supplementary Information*) shows the SEM images of the products obtained from 180 ℃ for 24 h using PVP with different concentrations. The products are totally composed of irregular particles with nanoscale and sub-microscale size when the experiment was performed using 0.1wt.% PVP (Figs. S3(a) and 3(b)). Upon adding 1wt.% PVP, some nanobelts with the length and width of about several tens of micrometers and 200 nm-1 μm, respectively are observed besides irregular particles (Figs. S3(c) and 3(d)). The results show that PVP has an important role in the formation of the copper vanadate nanobelts. The copper vanadate nanobelts are difficult to form without PVP, even adding a small amount of PVP which is similar to that reported by Li *et al*.[25] Other copper vanadate nanostructures, such as copper vanadate nanowires with α-CuV_2O_6 phase can be prepared

by the hydrothermal process using $CuCl_2$ and NH_4VO_3 as the raw materials without PVP.[14] Therefore, PVP has the important role in the formation of the copper vanadate nanobelts.

Fig. S4 (*Electronic Supplementary Information*) displays the morphological evolution of the copper vanadate nanobelts with the duration time. After 0.5 h, it is obviously observed that the products totally consist of nanosheets with the thickness and length of about 40 nm and 400 nm, respectively (Figs. S4(a) and 4(b)). With the duration time proceeding to 6 h, a small amount of nanobelts appear in the products besides nanosheets (Figs. S4(c) and 4(d)). The width and length of the nanobelts are 50-150 nm and 3 μm, respectively. With the duration time further extending to 12 h, a large number of copper vanadate nanobelts have been explosively formed (Figs. S4(e) and 4(f)) besides a small amount of nanosheets. The nanobelts have a length of several tens of micrometers and width of about 50 nm. The time-dependence results show that the duration time promotes the formation and growth of the copper vanadate nanobelts. The copper vanadate nanobelts grow from the nanosheets which is also confirmed by the subsequent temperature-dependent experiments. Hydrothermal temperature is also an important factor for the formation of the copper vanadate nanobelts. SEM images of the products obtained from 80 ℃ and 120 ℃ for 24 h with 3wt.% PVP and pH=2 are shown in Fig. S5 (*Electronic Supplementary Information*). It is obviously observed that a small amount of curved nanobelts with the length of 1 μm exist in the products besides irregular particles when the duration time is 80 ℃ (Figs. S5(a) and 5(b)). With the hydrothermal temperature extending to 120 ℃, the length of the copper vanadate nanobelts increases to 2 μm (Figs. S5(c) and 5(d)). Instead of irregular particles, the products are mainly composed of nanosheets besides nanobelts. Therefore, it is further confirmed that the copper vanadate nanobelts originate from the nanosheets.

Previous report showed that the copper vanadate nanowires with α-CuV_2O_6 phase could be obtained without surfactants by controlling the V and Cu raw materials under hydrothermal conditions.[14] Different

from the previous report, PVP was used in the present experiments. However, only copper vanadate rod-shaped morphology with nanoscale and sub-microscale size was obtained using PVP as the surfactant. Copper vanadate nanobelts have been obtained by controlling the hydrothermal solution with acidic or alkaline conditions. Therefore, pH value is considered to play an important role in the formation of the copper vanadate nanobelts. It is clear that the existence of hydrogen ions or hydroxyl ions accelerates the formation of the copper vanadate nanosheets.[19] In addition, PVP concentration, hydrothermal temperature and duration time have important roles in the formation of copper vanadate nanobelts. On the basis of the experimental results, it is supposed that the formation of the copper vanadate nanobelts can be ascribed to the copper vanadate nanosheets. The growth process of the copper vanadate nanobelts has been proposed based on the nucleation and PVP adsorption growth mechanism under acidic and alkaline conditions. Fig. 6 shows the PVP-assisted growth process shematic of the copper vanadate nanobelts. PVP belongs to non-ions surfactant and provides the coordination sites. The sites on the PVP molecules provide necessary heterogeneous nucleation sites. At the initial reaction stage, copper vanadate forms from the reaction between sodium vanadate and copper acetate. Therefore, copper vanadate clusters spontaneously appear in the supersaturated solution through the hydrothermal reaction between sodium vanadate and copper acetate. under acidic or alkaline hydrothermal conditons. The copper vanadate nanoclusters can serve as the heterogeneous nucleation sites for the formation of the copper vanadate nanosheets[26] which is confirmed by the analysis of PVP concentration, duration time and hydrothermal temperature on the formation of copper vanadate nanobelts. Under the acidic or alkaline hydrothermal solution, PVP is adsorbed at the surface of the copper vanadate nuclei inducing the formation of the copper vanadate nanosheets. The SEM images of the products obtained from short duration time and low hydrothermal temperature show the formation of a small amount of belt-shaped structures. The linear growth is mainly ascribed to the preferential adsorption

of PVP under acidic or alkaline hydrothermal solution which induces the growth of the nanosheets into nanobelts. The growth of the copper vanadate nanobelts with monoclinic $Cu_{2.33}V_4O_{11}$ phase is related to the anisotropic crystal structure of the monoclinic $Cu_{2.33}V_4O_{11}$. With increasing the hydrothermal temperature and duration time, copper vanadate nanobelts grow continuously. Sodium vanadate and copper acetate react totally leading in the final formation of the copper vanadate nanobelts with pure monoclinic $Cu_{2.33}V_4O_{11}$ phase.

It has been shown that ternary metal oxide 1D nanomaterials have attracted increasing attention because they can be used as the GCE modified materials for the electrochemical determination of biological molecules in recent years.[27] Among the biological molecules, ascorbic acid is widely used for the antioxidant properties, prevention and treatment of the common cold, mental illness, cancers, infertility and acquired immune deficiency syndrome (AIDS).[28-30] Therefore, it is essential to develop a simple and rapid method for the determination of ascorbic acid in the field of biomedical chemistry, neurochemistry and diagnostic research. Electrochemical method provides the advantages of fast and simple analysis process, high sensitivity, low detection limit, little or no sample preparation, simple operation and low cost.[31] The surface of the GCEs can be easily modified to enhance the sensitivity by the deposition of various layers, such as metal oxides and polymers.[18,32] In our previous research, ternary copper germanate nanowires were used as the GCE modified materials to investigate the electrochemical behaviors of ascorbic acid. The results showed that $CuGeO_3$ nanowires modified GCE exhibited good performance for the electrochemical detection of ascorbic acid in neutral solution.[17] The linear range was 0.01-5 mM and detection limit was 8.6 μM, respectively at a signal-to-noise ratio of 3. Copper vanadate nanobelts are considered to be used as the GCE modified materials for the analysis of biological molecules owing to high electrical conductivity, large specific surface area and chemical stability. It has been reported that copper vanadate could be employed as

the linker between the copper nanoparticles substrate and biological molecules for the determination of biological molecules, such as tyrosine and histidine by surface-enhanced Raman scatting (SERS) effect due to the interaction between copper vanadate and amino acids.[33] Copper vanadate nanobelts on the surface of the GCE may mediate the heterogeneous chemical oxidation or reduction of the target materials when the converted copper ions can be continuously recovered by the electrochemical oxidation or reduction process. Therefore, copper vanadate nanobelts are attempted to be used as the GCE modified materials for the electrochemical determination of ascorbic acid.

EIS is an effective tool for the analysis of the conductivity, electron transfer and interface properties of modified GCEs. Fig. 7 shows the EIS of the copper vanadate nanobelts modified GCE and bare GCE. The impedance spectrum of the copper vanadate nanobelts modified GCE is composed of a semicircle at high ac modulation frequency and a line at low ac modulation frequency. The results show that the copper vanadate nanobelts modified electrode process is controlled by the electron transfer process at high frequency and diffusion process at low frequency. The diameter of the Nyquist circle at the bare GCE is larger than that at the copper vanadate nanobelts modified GCE indicating that the copper vanadate nanobelts GCE has higher electrochemical activity and faster electron transfer on the surface than bare GCE. The result shows that the copper vanadate modified GCE can decrease the electron transfer resistance and improve the electron transfer process.

Fig. 8 shows the electrochemical responses of ascorbic acid at the bare GCE and copper vanadate nanobelts modified GCE in 0.1 M KCl with 2 mM ascorbic acid. No electrochemical CV peaks are observed from the electrochemical CV curve (Fig. 8(a)) at bare GCE showing that bare GCE has no electrochemical activity for ascorbic acid. The electrochemical CV curve of ascorbic acid at the copper vanadate nanobelts modified GCE is greatly different from that at the bare GCE. Two anodic CV peaks

(cvp1, cvp2) are located at 0.12 V and 0.02 V. Two cathodic CV peaks (cvp1′, cvp2′) are located at 0.04 V and -0.81 V, respectively (Fig. 8(b)). Some literatures have reported the electrochemical behaviors of ascorbic acid at the electrodes modified by different materials. Tyszczuk-Rotko *et al.*[34] reported the electrochemical behaviors of ascorbic acid at a GCE modified with Nafion and lead films in 0.1 M acetate buffer in the presence of 0.025 mM ascorbic acid. Only an irreversiblly anodic CV peak located at +0.04 V occurred from the CV curve. The electrochemical behaviors of ascorbic acid at disposable gold-based compact disks (G-CDs) electrodes modified by $[Mn(Phimp)_2](ClO_4)$ showed that only a rising of the anodic current was observed at a potential above 1.0 V.[31] No cathodic peak was observed due to the irreversiblity of the electrocatalytic process. Irreversible anodic CV peak was also observed at +0.523 V and +0.534 V from the CV curve of 0.5 mM ascorbic acid at the carbon nanotubes-N and Fe_3O_4@carbon nanotubes-N modified electrode, respectively.[32] Ma *et al.*[18] reported that a pair of semi-reversible electrochemical CV peaks located at +0.25 V and -0.40 V were observed from the electrothemical CV curve of 0.04 mM ascorbic acid at 3D gaphene-CuO modified GCE. Different from the irreversible CV peak and a pair of semi-reversible CV peaks reported from above literatures, two pairs of semi-reversible electrochemical CV peaks are observed. Two pairs of semi-reversible CV peaks were also observed from the CV curve of ascorbic acid at ternary copper germanate nanowires modified GCE.[35] Two anodic CV peaks (cvp1, cvp2) were located at +0.20 V and +0.02 V and two cathodic CV peaks (cvp1′, cvp2′) were located at +0.07 V and -0.41 V, respectively. The electrochemical CV peaks at the copper germanate nanowires modified GCE were assigned to the oxidation-reduction process (cvp1-cvp1′) and adsorption-desorption process (cvp2-cvp2′) between ascorbic and dehydroascorbic acid, respectively. The two pairs of electrochemical CV peaks at copper vanadate nanobelts modified GCE are similar to those of ascorbic acid at copper germanate nanowires modified GCE. Therefore, two pairs of semi-reversible CV

peaks at the copper vanadate nanobelts modified GCE are also due to the oxidation-reduction process (cvp1-cvp1′) and adsorption-desorption process (cvp2-cvp2′) between ascorbic acid and dehydroascorbic acid, respectively. In addition, two pairs of CV peaks of asorbic acid are only observed at the copper vanadate nanobelts modified GCE showing that the CV peaks originate from the copper vanadate nanobelts. The vast amount of active sites provided by copper vanadate nanobelts on the modified GCE can lower the energy barrier of the redox of ascorbic acid and act as the media to boost electron transfer between ascorbic acid in the solution and modified GCE because the oxidation of ascorbic acid is an inner-sphere reaction that is sensitive to the surface of the electrodes.[36] The whole oxidation process of ascorbic acid can be explained as follows. Ascorbic acid molecules are diffused to the nearest active sites and absorbed onto the surface of the copper vanadate nanobelts.[37] Then the absorbed ascorbic acid molecules are oxidized to dehydroascorbic acid catalyzed by the copper vanadate nanobelts.

The CVs of ascorbic acid at the copper vanadate nanobelts modified GCE using different initial potential scan direction and reversal potential were measured to analyze whether the anodic and cathodic peaks are semi-reversible process. The intensities of the CV peaks are similar when changing the initial potential scan direction. However, the intensities of the CV peaks vary by changing the reversal potential. Fig. 9 shows the CV curves of ascorbic acid at the copper vanadate nanobelts modified GCE using different reversal potentials. No electrochemical CV peaks are observed when initial reversal potential is +0.5 V, +0.3 V and +0.2 V, respectively which is higher than the potential of cvp1′. However, a pair of electrochemical CV peaks are observed with the initial reversal potential increasing to 0 V which is smaller than that of cvp1′. Therefore, cvp1 is the oxidation process of the products originated from the potential of cvp1′. The electrochemical CV peaks, cvp2 and cvp2′ are observed when the reversal potential reduces to -0.8 V. Therefore, it is concluded that the electrohcemical CV peaks, cvp1 and cvp2 originate from the CV

peaks of cvp1′ and cvp2′.

Fig. 10 shows the CVs of ascorbic acid in the mixed solution of 0.1 M KCl and 2 mM ascorbic acid using different scan rates. With the increase of the scan rate from 25 to 200 mVs^{-1}, the intensity of the electrochemical CV peaks increases obviously. The effect of the scan rate on the anodic oxidation current of ascorbic acid is also analyzed (inset in the bottom-left part of Fig. 10). There is a linear correlation between the anodic current and scan rate in the range of 25-200 mVs^{-1}. The correlation coefficient *R* is 0.995 and 0.987 for cvp1 and cvp2, respectively. The results suggest that the kinetic of the overall process is controlled by an adsorption process.[17,38,39] Therfore, the copper vanadate nanobelts play the key role which provides an ideal morphology for anchoring bioactive molecules and rapid pathway for mass transfer which is also similar to that reported by Ma *et al.*[18]

The linear range, correlation coefficient and detection limit of ascorbic acid at the copper vanadate nanobelts modified GCE were analyzed by investigating the CV curves of ascorbic acid with the concentration in the range of 0.001-2 mM (Fig. 11). The inset in the bottom-left part of Fig. 11 is the calibration plots of the intensities of the anodic peaks with the increase of the ascorbic acid concentration. The intensity of the CV peaks increases obviously with increasing the concentration of the ascorbic acid. Table 2 shows the analytical data of ascorbic acid with the linear range, detection limit and correlation coefficient. The linear range is 0.001-2 mM with the correlation coefficient *R* of 0.997 and 0.993 for cvp1 and cvp2, respectively. The linear range is defined as the concentration ranges that meet linearity criteria. The correlation coefficient (>0.99) of the linearity fit looks good and 0.001-2 mM is considered as the linear range. The detection limit is 0.14 μM and 0.38 μM for cvp1 and cvp2, respectively at a signal-to-noise ratio of 3. The comparison of the analytical performance of the electrochemical determination of ascorbic acid with other electrodes is shown in Table 3. It is noticed that the copper

vanadate nanobelts modified GCE has lowest detection limit for the electrochemical determination of ascorbic acid and a comparable linear range. Therefore, the copper vanadate nanobelts can be a potential biosensing platform for the electrochemical detection of ascorbic acid.

Electrochemical behaviors of ascorbic acid at the copper vanadate nanobelts modified GCE were investigated in various electrolytes, such as pbs (pH=7) and NaOH (pH=12), H_2SO_4 (pH=2) and CH_3COONa-CH_3COOH (pH=5). In neutral pbs solution, the electrochemical response of ascorbic acid (Fig. 12(a)) is similar to that in KCl solution. However, the intensities of the CV peaks vary slightly and the potentials of the anodic CV peaks shift to more negative direction indicating the better electrocatalytic performance. No electrochemical CV peaks are observed in NaOH solution (Fig. 12(b)) showing that the copper vanadate nanobelts have no electrochemical activities for ascorbic acid in NaOH solution. Different from the electrochemical behavior of ascorbic acid in neutral solution, a broad and strong anodic CV peak appears at +0.35 V when the electrochemical CV curve of ascorbic acid is obtained in H_2SO_4 electrolyte with pH value of 2 (Fig. 12(c)). The intensity of the electrochemical CV peaks is far larger than that in neutral solution. The electrochemical CV curve of ascorbic acid in CH_3COONa-CH_3COOH buffer solution with the pH value of 5 is shown in Fig. 12(d)). In the acidic solution, the electrochemical CV peak cvp1 overlaps with cvp2 leading in the formation of only one pair of broad redox CV peaks. The absorbed ascorbic acid molecules are considered to be oxidized to dehydroascorbic acid catalyzed by the copper vanadate nanobelts. Therefore, hydrogen ions in the solution with low pH value induce the electrochemical reaction of sscorbic acid to dehydroascorbic acid.

The long term stability and reproducibility of the copper vanadate nanobelts modified GCE were investigated. The copper vanadate nanobelts modified GCE was stored at room temperature for 1 month and can still be used for the determination of ascorbic acid without any decrease of the current response.

The copper vanadate nanobelts can be adsorbed firmly at the modified GCE. With the ascorbic acid with the concentration of 2 mM for twenty measurements, the relative standard deviation (R.S.D.) is found to be 4.93% and 5.34% for cvp1 and cvp2, respectively (Fig. 13). The results indicate that the copper vanadate nanobelts modified GCE has good stability and reproducibility for the electrochemical determination of ascorbic acid.

D Conclusions

In summary, single crystalline copper vanadate nanobelts with monoclinic $Cu_{2.33}V_4O_{11}$ phase, thhickness of 50 nm, width of 300 nm-1 μm and length of several tens of micrometers have been synthesized by a simple and facile hydrothermal process using sodium vanadate and copper acetate as the raw materials, PVP as the surfactant by adjusting the pH value. pH value plays a key role in the formation and growth of the copper vanadate nanobelts. Hydrothermal temperature, duration time and PVP concentration have important effects in the formation, size and morphology of the copper vanadate products. The nucleation and PVP adsorption growth mechanism under acidic and alkaline conditions have been proposed to explain the formation and growth of the copper vanadate nanobelts. The copper vanadate nanobelts have been used as the GCE modified materials for the electrochemical determination of ascorbic acid. The electrochemical behaviors of ascorbic acid at the copper vanadate nanobelts modified GCE show that two pairs of semi-reversible electrochemical peaks are observed. The linear range is 0.001-2 mM and detection limit is 0.14 μM and 0.38 μM for cvp1 and cvp2, respectively. The copper vanadate nanobelts modified GCE exhibits good stability and reproducibility. The copper vanadate nanobelts show the promising potential for the electrochemical determination of ascorbic acid or other biological molecules.

Acknowledgments

This work was supported by the Innovative Research Foundation of Postgraduate of Anhui University of

Technology (2014077) and Natural Science Foundation of Anhui Province (1208085QE98).

Tables

Table 1 Experimental parameters of the products synthesized from different pH value, PVP concentration, hydrothermal temperature and duration time

Raw materials	PVP concentration (wt.%)	pH value	Temperature (℃)	Duration time (h)	Product morphology
Sodium vanadate and copper acetate	3	2	180	24	Nanobelts
	3	5	180	24	Nanobelts
	3	7	180	24	Microrods
	3	9	180	24	Nanobelts
	3	12	180	24	Nanobelts
	0.1	2	180	24	Irregular particles and a small amount of nanobelts
	1	2	180	24	Irregular particles and nanorods
	3	2	180	0.5	Nanosheets
	3	2	180	6	Nanosheets and a small amount of nanobelts
	3	2	180	12	Nanobelts and a small amount of nanosheets
	3	2	80	24	Irregular particles and a small amount of nanobelts
	3	2	120	24	Nanosheets and a small amount of nanobelts

Table 2 Analytical data of the ascorbic acid

CV peaks	Regression equation[a]	Correlation coefficient (R)	Linear range (mM)	Detection limit (μM) [b]
cvp1	I_p=20.818+68.191C	0.997	0.001-2	0.14
cvp2	I_p=22.429+47.035C	0.993	0.001-2	0.38

[a] Where I_p and C represent the peak current (μA) and the concentration of the ascorbic acid (mM)

[b] The detection limit of the ascorbic acid was analyzed using a signal-to-noise ratio of 3 (S/N=3)

Table 3 Comparison of analytical performance of the electrochemical determination of ascorbic acid with other electrodes

Electrodes	Linear range (mM)	Detection limit (μM)	Ref.
Copper germanate/polyaniline nanowires	0.001-2	0.26	[17]
3D graphene foam/CuO nanoflowers	0.00043-0.2	0.43	[18]
Multi-walled carbon nanotubes bridged mesocellular graphene foam nanocomposites modified GCE	0.1-6	18.28	[28]
Fe_3O_4@N-doped CNTs	0.005-0.235	0.24	[32]
Copper germanate nanowires	0.01-5	8.6	[35]
Molecularly imprinted polypyrrole-modified pencil graphite	0.25-7	74	[40]
Polymerized direct blue 71 (DB71) nanoparticles	0.001-2	1	[41]
$Cu_4(OH)_6SO_4$ nanorods	0.017-6	6.4	[42]
γ-MnO_2	0.001-4	0.6	[43]
Cellulose acetate film bearing 2,6-dichlorophenolindophenol	0.02-1	10	[44]
GCE/MWCNTs-polyhis	0.25-2.5	0.76	[45]
Pd nanowire modified GCE	0.25-0.9	0.2	[46]
Graphene/Pt modified GCE	0.00015-0.0344	0.15	[47]
Ni-Pt alloys	0.57-5.68	570	[48]
Fe_3O_4/graphene oxide sheets	0.16-7.2	20	[49]
Screen printed graphene	0.004-4.5	0.95	[50]
Gr flowers modified CF	0.0454-1.48923	24.7	[51]
OPPy-PdNPs/Au	0.001-0.52	1	[52]
Copper vanadate nanobelts	0.001-2	0.14	Current work

Notes and references

1. L. Z. Pei, S. Wang, H. D. Liu and Y. Q. Pei, *Recent Pat. Nanotechnol.*, 2014, **8**, 142.

2 Y. Wang and G. Z. Cao, *J. Mater. Chem.*, 2007; **17**, 894.

3 R. D. Holtz, A. G. S. Filho, M. Brocchi, D. Martins, N. Durán and O. L. Alves, *Nanotechnology*, 2010, **21**, 185102.

4 J. Q. Yu and A. Kudo, *Chem. Lett.*, 2005, **34**, 850.

5 L. Z. Pei, Y. Q. Pei, Y. K. Xie, C. Z. Yuan, D. K. Li and Q. F. Zhang, *CrystEngComm*, 2012, **14**, 4262.

6 L. Z. Pei, Y. K. Xie, Y. Q. Pei, Y. X. Jiang, H. Y. Yu and Z. Y. Cai, *Mater. Res. Bull.*, 2013, **48**, 2557.

7 W. D. Huang, S. K. Gao, X. K. Ding, L. L.l Jiang and M. D. Wei, *J. Alloys Compd.*, 2010; **495**, 185.

8 D. P. Singh, K. Polychronopoulou, C. Rebholz and S. M. Aouadi, *Nanotechnology*, 2010; **21**, 325601.

9 W. W. Li, Q. Wang, W. S. You, L. J. Qi, L. M. Dai and Y. Fang, *Inorg. Chem. Commun.*, 2009, **12**, 1185.

10 X. Y. Cao, J. G. Xie, H. Zhan and Y. H. Zhou, *Mater. Chem. Phys.*, 2006, **98**, 71.

11 Y. J. Wei, K. W. Nam, G. Chen, C. W. Ryu and K. B. Kim, *Solid State Ionics*, 2005, **176**, 2243.

12 W. Hu, X. C. Du, Y. M. Wu and L. M. Wang, *J. Power Sources*, 2013, **237**, 112.

13 G. C. Li, W. Z. Wu, C. Q. Zhang, H. R. Peng and K. Z. Chen, *Mater. Lett.*, 2010, **64**, 820.

14 H. Ma, S. Zhang, W. Ji, Z. Tao and J. Chen, *J. Am. Chem. Soc.*, 2008, **130**, 5361-5367.

15 L. Z. Pei, Y. Q. Pei, Y. K. Xie, C. G. Fan and H. Y. Yu, *CrystEngComm*, 2013, **15**, 1729.

16 L. Z. Pei, Y. Q. Pei, Y. K. Xie, C. G. Fan, D. K. Li and Q. F. Zhang, *J. Mater. Res.*, 2012, **27**, 2391.

17 L. Z. Pei, Z. Y. Cai, Y. K. Xie, Y. Q. Pei, C. G. Fan and D. G. Fu, *J. Electrochem. Soc.*, 2012, 159, G107.

18 Y. Ma, M. G. Zhao, B. Cai, W. Wang, Z. Z. Ye and J. Y. Huang, *Biosens. Bioelectr.*, 2014, **59**, 384.

19 X. Z. Zeng, X. Zhang, M. Yang and Y. X. Qi, *Mater. Lett.*, 2013, **112**, 87.

20 Y. F. Zhang, C. X. Chen, W. B. Wu, F. Niu, X. H. Liu, Y. L. Zhong, Y. L. Cao, X. Liu and C. Huang, *Ceram. Int.*, 2013, **39**, 129.

21 L. Li, J. Liang, M. Luo and J. Z. Fang, *Powder Technol.*, 2012, **226**, 143.

22 A. Phuruangrat, J. S. Chen, X. W. Lou, O. Yayapao, S. Thongtem and T. Thongtem, *Appl. Phys. A*, 2012, **107**, 249.

23 Y. F. Zhang, M. J. Fan, X. H. Liu, G. Y. Xie, H. B. Li and C. Huang, *Solid State Commun.*, 2012, **152**, 253.

24 S. Y. Zhang, R. S. Hu, L. Liu and D. Y. Wang, *Mater. Lett.*, 2014, **124**, 57.

25 Z. J. Luo, H.l M. Li, J. X. Xia, W. S. Zhu, J. X. Guo and B. B. Zhang, *Mater. Lett.*, 2007, **61**, 1845.

26 R. C. Rao, M. Yang, Q. Ling, Q. Y. Zhang, H. D. Liu, A. M. Zhang and W. Chen, *Micopor. Mesopor. Mat.*, 2013, **169**, 81.

27 Y. P. Dong, L. Z. Pei, X. F. Chu and Q. F. Zhang, *Electrochim. Acta*, 2010, **7**, 5135.

28 H. X. Li, Y. Wang, D. X. Ye, J. Luo, B. Q. Su, S. Zhang and J. L. Kong, *Talanta*, 2014, **127**, 255.

29 S. J. Yu, C. H. Luo, L. W. Wang, H. Peng and Z. Q. Zhu, *Analyst*, 2013, **138**, 1149.

30 X. Q. Tian, C. M. Cheng, H. Y. Yuan, J. Du, D. Xiao, S. P. Xie and M. M. F. Choi, *Talanta*, 2012, **93**, 79.

31 S. G. Leonardi, D. Aloisio, N. Donato, S. Rathi, K. Ghosh and G. Neri, *Mater. Lett.*, 2014, **133**, 232.

32 D. M. Fernandes, M. Costa, C. Pereira, B. Bachiller-Baeza, I. Rodríguez-Ramos, A. Guerrezo-Ruiz and C. Freire, *J. Colloid Interf. Sci.*, 2014, **432**, 207.

33 H. Y. Lin, Q. Shao, F. Hu, H. Wang and M. W. Shao, *Thin Solid Films*, 2014, **558**, 385.

34 K. Tyszczuk-Rotko, I. Beczkowska, M. Wójciak-Kosior and I. Sowa, *Talanta*, 2014, **129**, 384.

35 L. Z. Pei, Y. K. Xie, Z. Y. Cai, Y. Yang, Y. Q. Pei, C. G. Fan and D. G. Fu, *J. Electrochem. Soc.*, 2012, **159**, K55.

36 G. Wu, Y. Wu, X. Liu, M. Rong, X. Chen and X. Chen, *Anal. Chim. Acta*, 2012, **745**, 33.

37 D. P. Dubal, G. S. Gund, R. Holze and C. D. Lokhande, *J. Power Sources*, 2013, **242**, 687.

38 N. Sehlotho and T. Nyokong, *Electrochim. Acta*, 2006, **51**, 4463.

39 J. Davis, M. Moorcroft, S. J. Wilkins, R. G. Compton and M. F. Cardosi, *Analyst*, 2000**, 125**, 737.

40 L. Özcan, M. Sahin and Y. Sahin, *Sensor.*, 2008, **8**, 5792.

41 S. A. Kumar, P. H. Lo and S. M. Chen, *Biosens. Bioelectron.*, 2008, **24**, 518.

42 C. Xia and W. Ning, *Analyst*, 2011, **136**, 288.

43 J. Zhang, P. H. Deng, Y. L. Feng, Y. F. Kuang and J. J. Yang, *Microchim. Acta*, 2004, **147**, 279.

44 A. B. Florou, M. I. Prodromidis, M. I. Karayannis and S. M. Tzouwara-Karayanni, *Anal. Chim. Acta*, 2000, **409**, 113.

45 P. R. Dalmasso, M. L. Pedano and G. A. Rivas, *Sens. Actuators B: Chem.*, 2012, **173**, 732.

46 D. Wen, S. Guo, S. Dong and E. Wang, *Biosens. Bioelectron.*, 2010, **26**, 1056.

47 C. Sun, H. Lee, J. Yang and C. Wu, *Biosens. Bioelectron.*, 2011, **26**, 3450.

48 Y. C. Weng, Y. G. Lee, Y. L. Hsiao and C. Y. Lin, *Electrochim. Acta*, 2011, **56**,9937.

49 H. Teymourian, A. Salimi and S. Khezrian, *Biosens. Bioelectron.*, 2013, **49**, 1.

50 J. Ping, J. Wu, Y. Wang and Y. Ying, *Biosens. Bioelectron.*, 2012, **34**, 70.

51 J. Du, R. Yue, E. Ren, Z. Yao, F. Jiang and P. Yang, *Biosens. Bioelectron.*, 2014, **53**, 220.

52 W. Shi, C. Liu, Y. Song, N. Lin, S. Zhou and X. Cai, *Biosens. Bioelectron.*, 2012, **38**, 100.

Figure captions

Fig. 1 XRD pattern of the copper vanadate nanobelts.

Fig. 2 SEM images of the copper vanadate nanobelts with different magnifications obtained from 180 ℃ for 24 h with the pH value of 2 using 3wt.% PVP as the surfactant, copper acetate and sodium vanadate as the raw materials.

Fig. 3 Transmission electron microscopy images of the copper vanadate nanobelts. (a) TEM image, (b) HRTEM image.

Fig. 4 SEM images of the copper vanadate products obtained from 180 ℃ for 24 h with different pH values and 3wt.% PVP using copper acetate and sodium vanadate as the raw materials. (a) and (b) pH=5, (c) and (d) pH=9, (e) and (f) pH=12.

Fig. 5 XRD patterns of the copper vanadate products synthesized from 180 ℃ for 24 h with different pH values and 3wt.% PVP using copper acetate and sodium vanadate as the raw materials. (a) pH=2, (b) pH=5, (c) pH=7, (d) pH=9, (e) pH=12.

Fig. 6 The growth process shematic of the copper vanadate nanobelts.

Fig. 7 EIS of bare GCE and copper vanadate nanobelts modified GCE. $K_3Fe(CN)_6$, 1 mM, KCl, 0.1 M.

Fig. 8 CVs of the copper vanadate nanobelts modified GCE in 0.1 M KCl solution in absence (a) and presence (b) of 2 mM ascorbic acid. Scan rate, 50 mVs^{-1}.

Fig. 9 Effect of the reverse potential on the electrochemical responses of ascorbic acid at the copper vanadate nanobelts modified GCE. KCl, 0.1 M, ascorbic acid, 2 mM, scan rate, 50 mVs^{-1}.

Fig. 10 CVs of the copper vanadate nanobelts modified GCE in the mixed solution of 0.1 M KCl and 2 mM ascorbic acid using different scan rates. The inset in the bottom-left part is the calibration plots of the intensities of anodic peaks against the scan rate.

Fig. 11 CVs of the ascorbic acid with different concentrations at the copper vanadate nanobelts modified GCE. KCl, 0.1 M, scan rate, 50 mVs^{-1}. The inset in the bottom-left part is the calibration plots of the intensities of the anodic peaks against the ascorbic acid concentration.

Fig. 12 CVs of the copper vanadate nanobelts modified GCE in the mixed solution of 2 mM ascorbic acid and different electrolytes. Scan rate, 50 mVs^{-1}. (a) pbs, (b) NaOH, (c) H_2SO_4, (d) CH_3COONa-CH_3COOH.

Fig. 13 CVs of the copper vanadate nanobelts modified GCE in the mixed solution of 0.1 M KCl and 2 mM ascorbic acid recycling for the 1st and 20th time, respectively. Scan rate, 50 mVs^{-1}.

Figures

Fig. 1

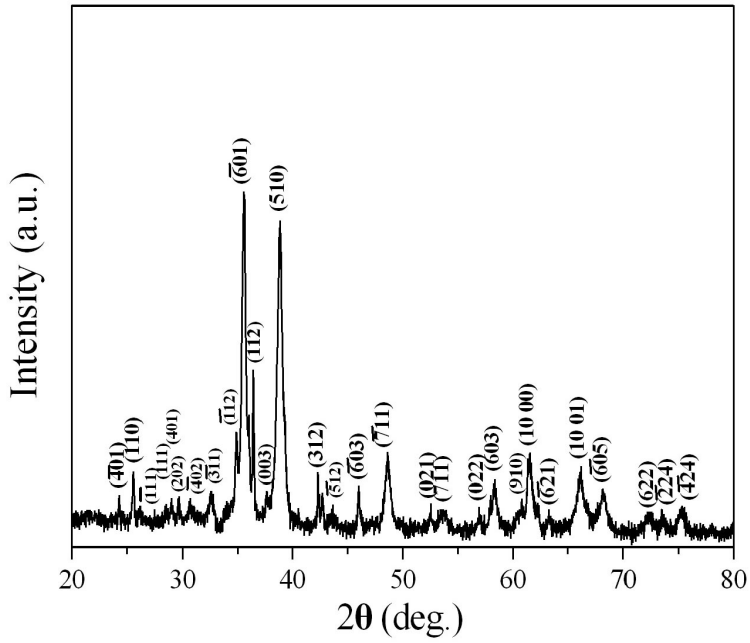

Fig. 2

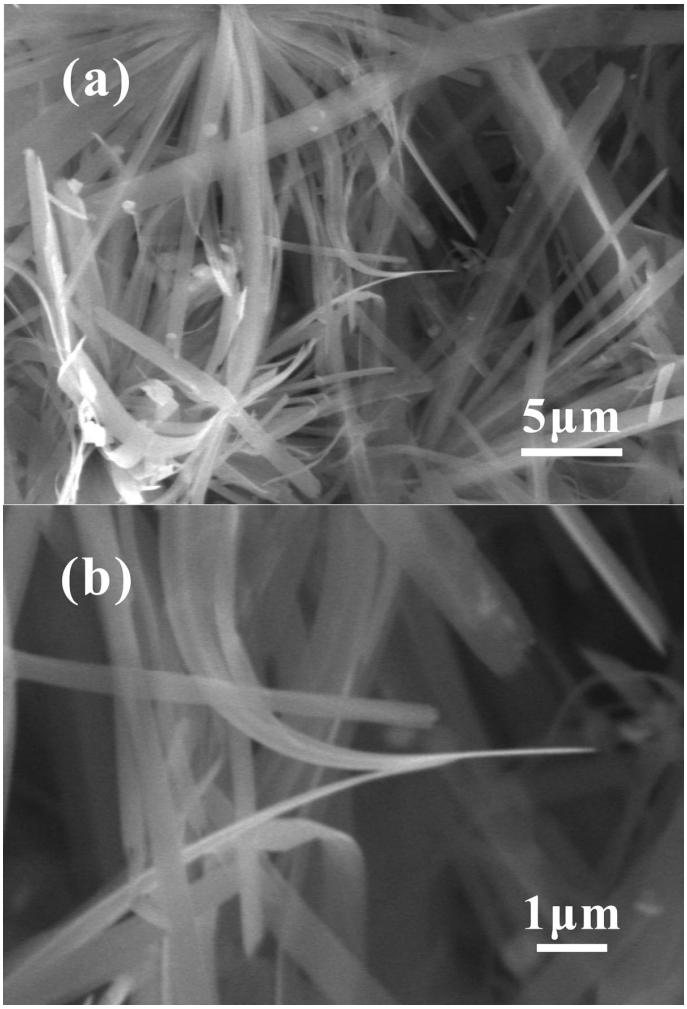

Fig. 3

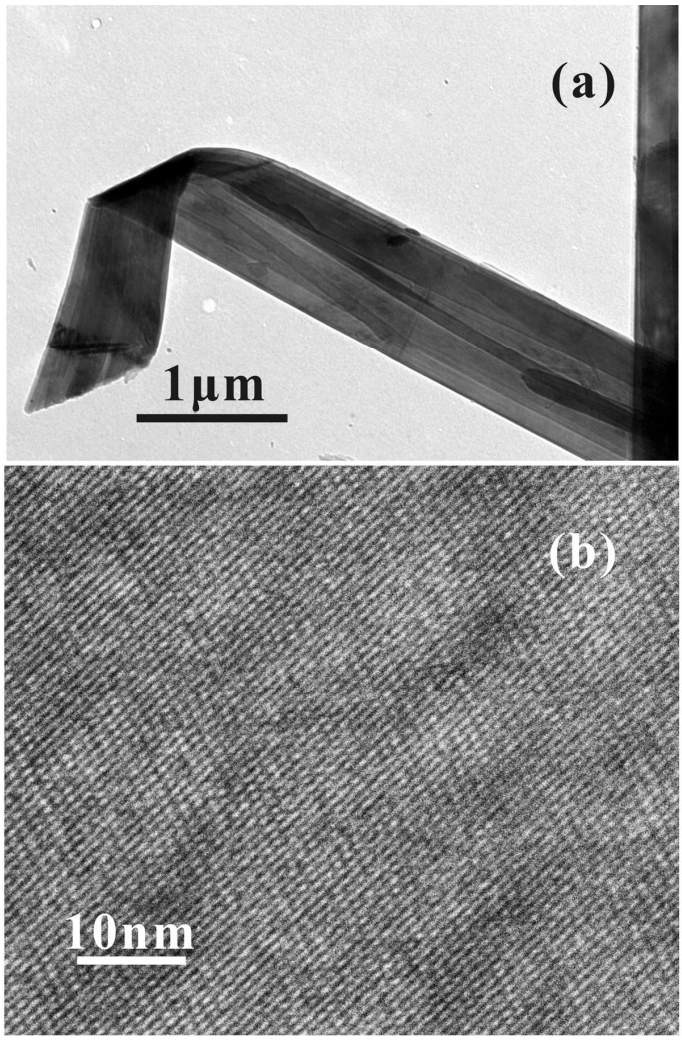

Fig. 4

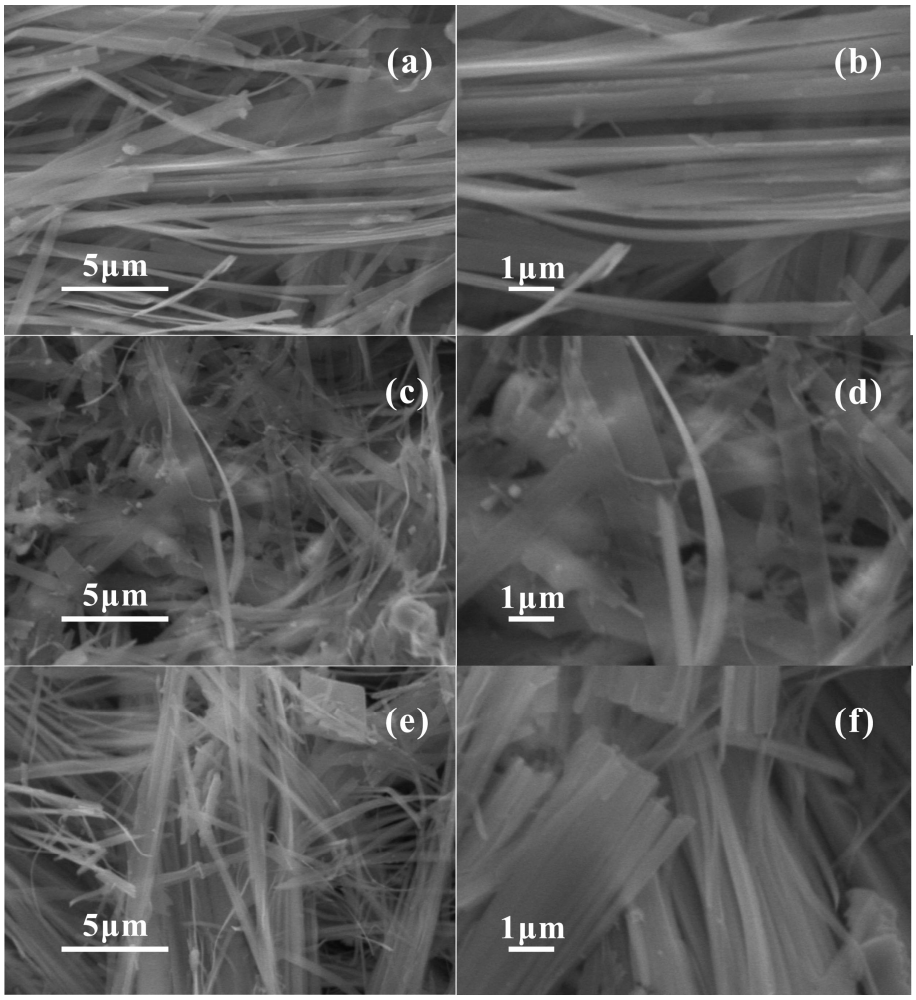

Fig. 5

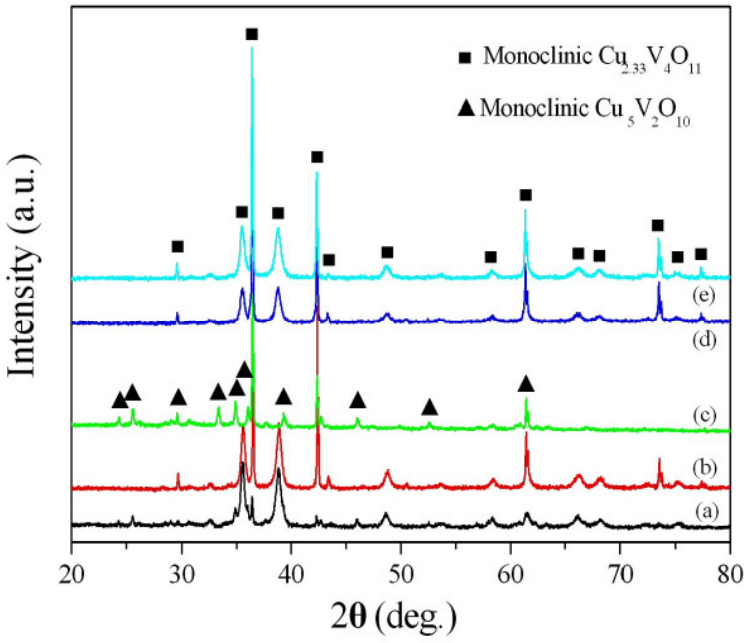

Fig. 6

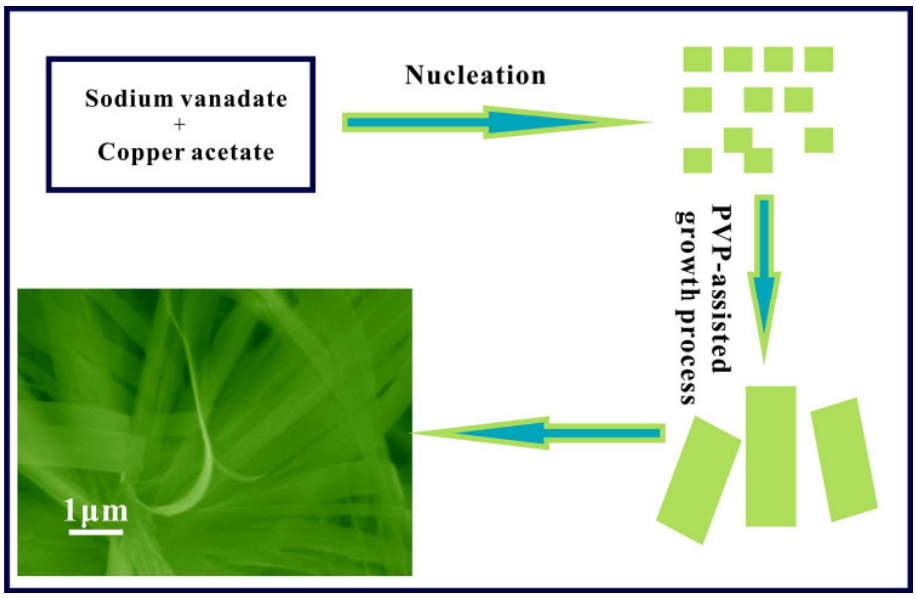

Fig. 7

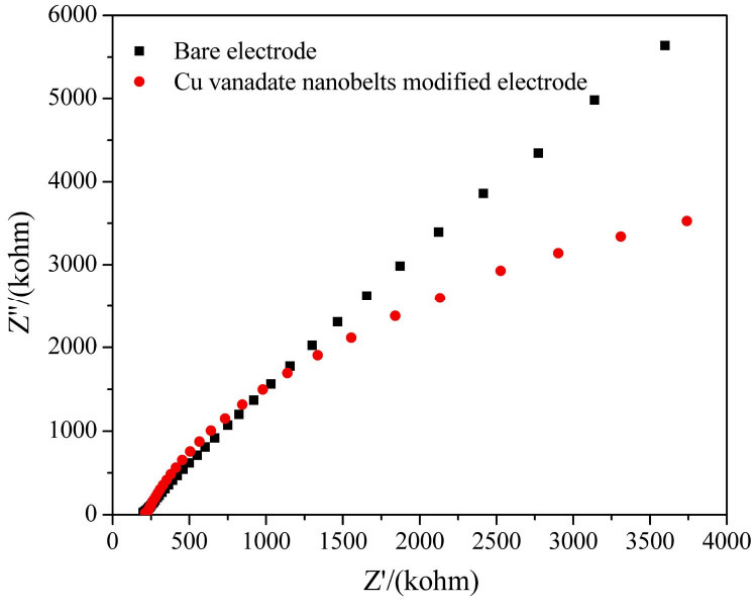

Fig. 8

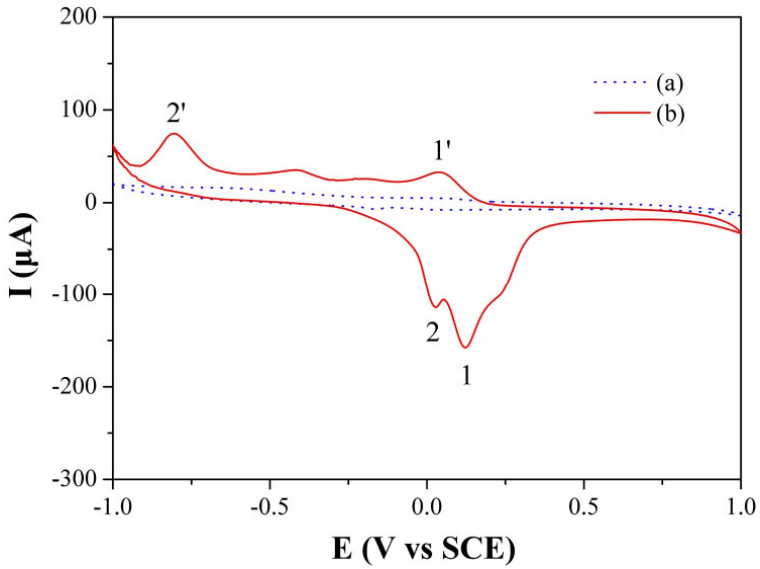

Fig. 9

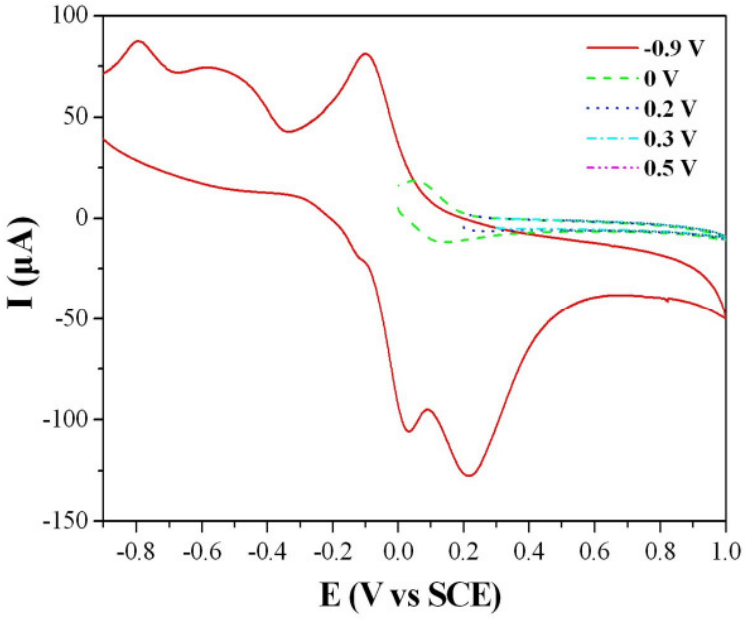

Fig. 10

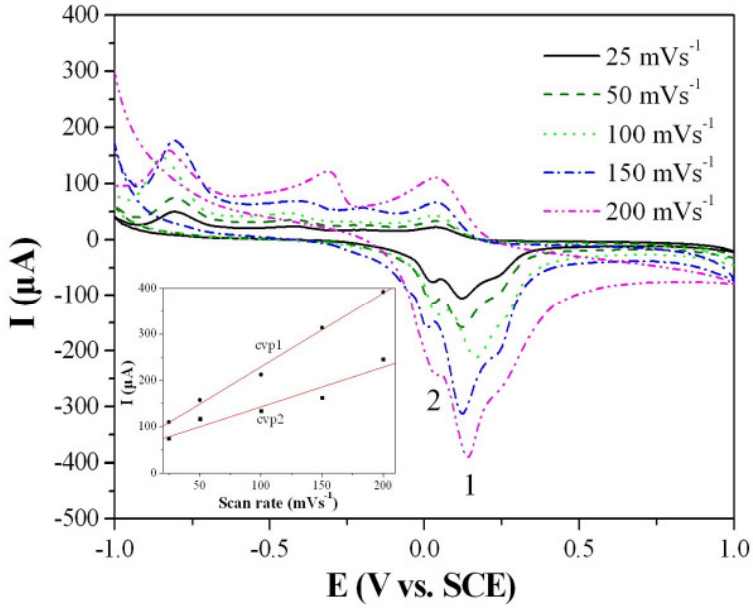

Fig. 11

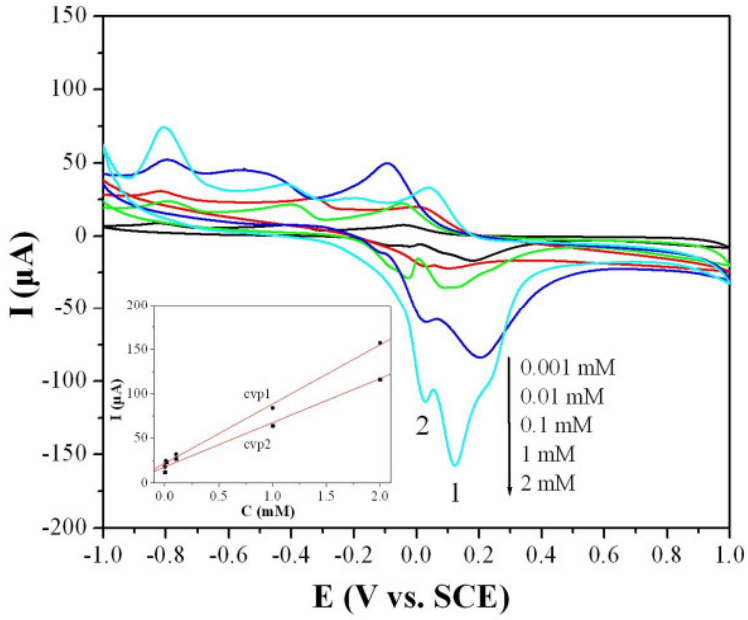

Fig. 12

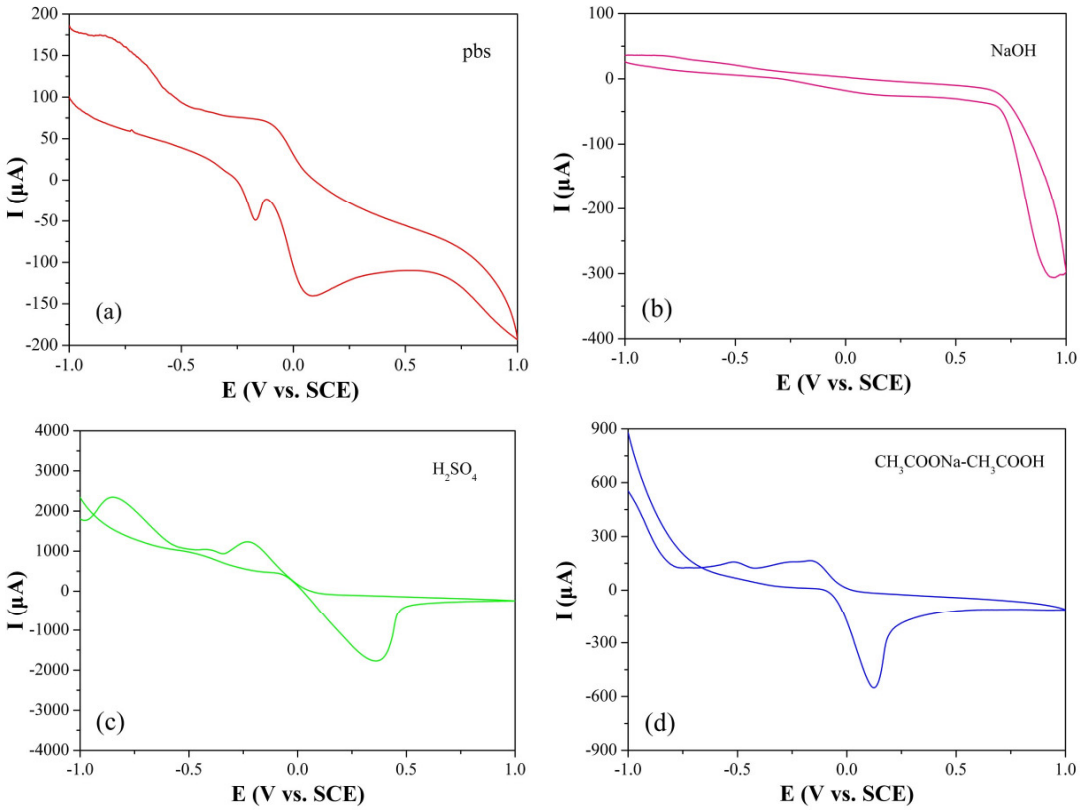

Fig. 13

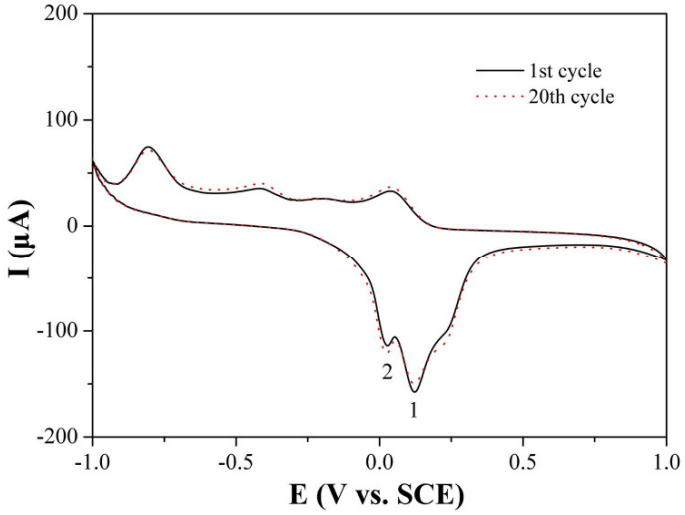

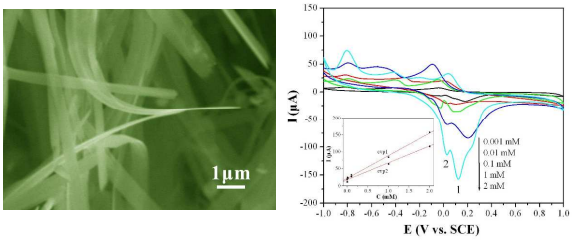

Copper vanadate nanobelts were synthesized by a facile hydrothermal process and used for the electrochemical determination of ascorbic acid.